Acta Neuropathol (2005) 109: 632–638
DOI 10.1007/s00401-005-1017-5

REGULAR PAPER

Yasushi Iwasaki · Mari Yoshida · Manabu Hattori
Yoshio Hashizume · Gen Sobue

Widespread spinal cord involvement in corticobasal degeneration

Received: 16 November 2004 / Revised: 16 February 2005 / Accepted: 16 February 2005 / Published online: 26 May 2005

Abstract We examined spinal cord lesions in eight patients with a pathological diagnosis of corticobasal degeneration (CBD). Using Gallyas-Braak (G-B) staining or AT-8 tau immunostaining, a few neuropil threads were identified in the white matter of the CBD spinal cords, mainly in the anterior funiculus, whereas the posterior funiculus was well preserved without threads. In the gray matter of the CBD spinal cords, particularly in the intermediate gray matter, there were widespread neuropil threads and neuronal inclusions. Large motor neurons in the anterior horn, neurons in the intermediolateral column, and Clarke's column were relatively well preserved from neuronal loss and gliosis. Neuronal inclusions were of the globose type, suggestive of neurofibrillary tangles (NFTs), or showed diffuse granular accumulations of cytoplasmic tau, suggestive of pretangles. No typical NFTs, recognized by Bodian silver staining, were identified. The distribution of neuropil threads and G-B- or AT-8 tau-positive small neurons resembled that of interneurons. No astrocytic plaques were present in any of the CBD spinal cords, and only a few coiled bodies were seen. Neuropil threads in the white and gray matter and neuronal inclusions in the gray matter were prominent in cervical segments, and their density decreased caudally. We suggest that the presence of neuropil threads, particularly in the cervical intermediate gray matter, and the presence of neuronal inclusions, particularly in cervical interneurons, is an essential pathological feature of CBD.

Keywords Corticobasal degeneration · Spinal cord lesion · Neuronal inclusion · Neuropil threads · Tau

Y. Iwasaki (✉) · G. Sobue
Department of Neurology,
Nagoya University Graduate School of Medicine,
65 Tsurumai-cho, Showa-ku, 466-8550 Nagoya, Japan
E-mail: iwasaki@sc4.so-net.ne.jp
Tel.: +81-52-7442391
Fax: +81-52-7442394

M. Yoshida · Y. Hashizume
Department of Neuropathology,
Institute for Medical Science of Aging,
Aichi Medical University, Aichi, Japan

M. Hattori
Department of Neurology and Neuroscience,
Nagoya City University Graduate School of Medical Science,
Nagoya, Japan

Introduction

Corticobasal degeneration (CBD) was first described as a novel neurodegenerative condition, termed corticodentatonigral degeneration with neuronal achromasia, by Rebeiz et al. [13] in 1968. Later, Gibb et al. [4] adopted the shorter name, CBD. CBD is a rare, sporadic disorder that occurs late in life, and is characterized clinically by disturbances in voluntary movement, which include 'alien hand', impaired ocular movement, dementia, aphasia, apraxia, and asymmetrical motor dysfunction in the extremities [3, 4, 5, 10, 13, 14, 18]. Extrapyramidal signs consist of various kinds of involuntary movement, akinesia, limb dystonia, and rigidity of the extremities [3, 4, 5, 10, 13, 14, 18]. It is generally difficult to diagnose CBD on the basis of clinical signs and symptoms [5], and accuracy of clinical diagnosis is, at present, low [5, 10]. The neuropathological hallmarks of CBD have been described as frontoparietal atrophy, the presence of ballooned neurons, i.e., neuronal achromasia in the cerebral cortex, and degeneration of the cerebral cortex and subcortical nuclei, particularly the substantia nigra [2, 4, 12, 13, 14, 18]. Although the pathophysiological mechanisms underlying these lesions are not completely understood, CBD is considered a discrete clinicopathological entity [2, 5, 13, 18].

There have been very few reports on the spinal cord lesions in CBD, and the pathological findings have been only briefly described [8, 11, 13, 18]. Thus, we examined the spinal cord lesions in eight CBD patients using Gallyas-Braak (G-B) staining [1, 6] and AT-8 tau immunohistochemistry.

Materials and methods

Specimens obtained at autopsy from eight patients with CBD from the Institute for Medical Science of Aging, Aichi Medical University, were included in the present study. Control spinal cords were collected from five patients judged to be free from degeneration following pathological examination and who did not have neurological symptoms. The CBD patients included seven men and one woman (mean age at death 68.3 ± 7.4 years, range 59–83 years), and the controls one man and four women (mean age at death 73.0 ± 2.0 years, range 71–76 years). The disease duration in the CBD patients ranged from 3 to 6 years (mean 4.1 ± 1.0 years). Asymmetric motor dysfunction in the extremities, which is characteristic of CBD, was recognized clinically in five of the eight CBD patients. Clinical data for the CBD patients, arranged in order of duration of illness, are summarized in Table 1. The neuropathological diagnosis of CBD was based on the presence of degeneration with ballooned achromatic neurons and astrocytic plaques in the cerebral cortices and basal ganglia, including the substantia nigra [2, 4, 5, 10, 13, 15]. Marked deposition of abnormal tau and argyrophilic structures in the neuropil, neurons, and glial cells in the cerebrum were noted in all eight CBD patients. Astrocytic plaques, a disease-specific hallmark of CBD [5], were also identified in the cerebral cortex in all patients. Seven of the eight CBD patients were included in a previous report regarding the preferential distribution of astrocytic plaques in the brain [5].

The entire spinal cord of each patient was fixed in 20% neutral-buffered formaldehyde. After fixation, the specimens were embedded in paraffin, and 8-μm-thick horizontal sections were prepared. The sections were mounted, deparaffinized, dehydrated, and stained as follows. For routine neuropathological study, spinal cord sections were subjected to hematoxylin and eosin (H-E), Holzer, Bodian, Klüver-Barrera (K-B), and G-B staining [1, 6]. Immunohistochemistry was carried out with an anti-paired helical filament (PHF)-tau monoclonal antibody (AT-8, 1:3,000; Innogenetics, Ghent, Belgium) by the labeled streptavidin-biotin (LSAB) method with a DAKO LSAB kit (DAKO, Glostrup, Denmark). For immunostaining, nonspecific endogenous peroxidase was blocked by pretreatment with 3% H_2O_2 for 10 min. The sections were then incubated with primary antibody overnight at 4°C. After washing, they were incubated with a biotinylated secondary antibody for 20 min. After another washing, the sections were incubated with peroxidase-conjugated streptavidin for 20 min. Peroxidase was visualized with 0.02% 3,3'-diaminobenzidine (WAKO Pure Chemical Industries, Osaka, Japan) as the final chromogen. Counterstaining with Mayer's hematoxylin was performed to stain cell nuclei.

The presence of neuronal loss was assessed by H-E and K-B staining. The presence of gliosis was evaluated by H-E and Holzer staining. Neurofibrillary tangles (NFTs) were identified by Bodian silver staining. G-B staining and AT-8 tau immunostaining were used to identify neuronal inclusions, including globose-type inclusions and pretangles, glial fibrillary tangles (GFTs), including astrocytic plaques and coiled bodies, and neuropil threads. We assayed sections at various spinal cord levels, including at least 6 cervical segments (C2–C7), at least 12 thoracic segments (T1–T12), and at least 6 lumbosacral segments (L1–S4). At each level, we examined tissue sections at x100 magnification and performed semiquantitative analysis of G-B-stained sections. Neuropil threads in the white and gray matter were counted semiquantitatively by density as: −, none; ±, few; +, slight; + +, moderate; or + + +, numerous per ×100 field in a unilateral region of interest (ROI). Neuronal inclusions in the gray matter were counted in the ROIs at

Table 1 Clinical summary of eight CBD autopsy cases (*AB* abnormal behavior, *Ag* agnosia, *Ak* akinesia, *Ap* apraxia, *Bk* bradykinesia, *CBD* corticobasal degeneration, *Da* dysarthria, *Dt* dystonia, *EM* eye movement, *GD* gait disturbance, *Ha* hallucination, *IS* instability upon standing, *IVM* involuntary movement, *Lt* left, *N.A.* not available, *ND* nuchal dystonia, *Rt* right, *Tr* tremor, *VP* vertical gaze palsy)

Patient	Age/sex	Disease duration (years)	Brain weight (g)	Initial symptom	EM disturbance	Laterality of clinical signs	Alien hand	Rigidity in extremities	Dementia	Other clinical signs
1	61/M	3	1,250	Rt hand clumsiness	+	+ Rt	+ Rt	+ Rt	–	GD, Da, Ag, Ak, Ap
2	72/M	3	1,220	GD	+	+ Rt	–	+	+	Da
3	65/M	4	1,315	Bk	+ VP	–	–	+	+	GD, AB, IS, Ak, Ha
4	68/M	4	1,350	GD	+ VP	+ Lt	–	+	+	Dt, Da
5	69/M	4	N.A.	Bk	+ VP	–	–	–	+	Memory loss, Ak, ND
6	69/M	4	1,110	GD	–	–	–	+	+	Bk, lethargy, Ak, IS
7	59/M	5	1,260	Lt leg weakness	–	+ Lt	–	+	+	Da
8	83/F	6	955	Rt hand Tr	+ VP	+ Rt	+ Rt	+ Rt	–	Dt, GD, Ap, IVM, Tr

all spinal levels and averaged as: −, absent; ±, 0–1 neuronal inclusion; +, 1–3 neuronal inclusions; + +, 3–6 neuronal inclusions; + + +, more than 6 neuronal inclusions. The ROIs were set for the white matter lesions as: anterior funiculus, lateral funiculus, and posterior funiculus; and for the gray matter lesions as: anterior horn, intermediate gray matter, and posterior horn.

Results

Macroscopic findings

Macroscopic appearances of the CBD spinal cords were unremarkable, and no atrophy was found.

Microscopic findings

White matter lesions

Pale or loose regions were not identifiable in horizontal spinal sections by K-B staining. A few to several neuropil threads were identified in five CBD patients by G-B staining (Fig. 1A) or AT-8 tau immunostaining (Fig. 1B). Detection of neuropil threads in the cervical white matter by G-B staining is summarized in Table 2A. Although neuropil threads in the white matter varied in density from patient to patient, they were identified predominantly in the marginal areas of the anterior horn, particularly in the anterolateral fasciculus, medial longitudinal fasciculus, and reticular formation. These findings were more prominent in the cervical segments than in the thoracolumbosacral segments and decreased in density caudally. All CBD samples lacked abnormal tau accumulation or argyrophilic structures in the posterior funiculus.

Gray matter lesions

Mild gliosis was present in some CBD samples, particularly in the medial division of the anterior horn and intermediate gray matter of cervical segments. The numbers of large motor neurons in the anterior horn were relatively unchanged. Neurons in the intermediolateral column were also relatively well preserved, and neurons in Clarke's column were well preserved from neuronal loss and gliosis.

G-B staining and AT-8 tau immunostaining revealed the presence of neuropil threads and neuronal inclusions in the gray matter (summarized for G-B staining in the

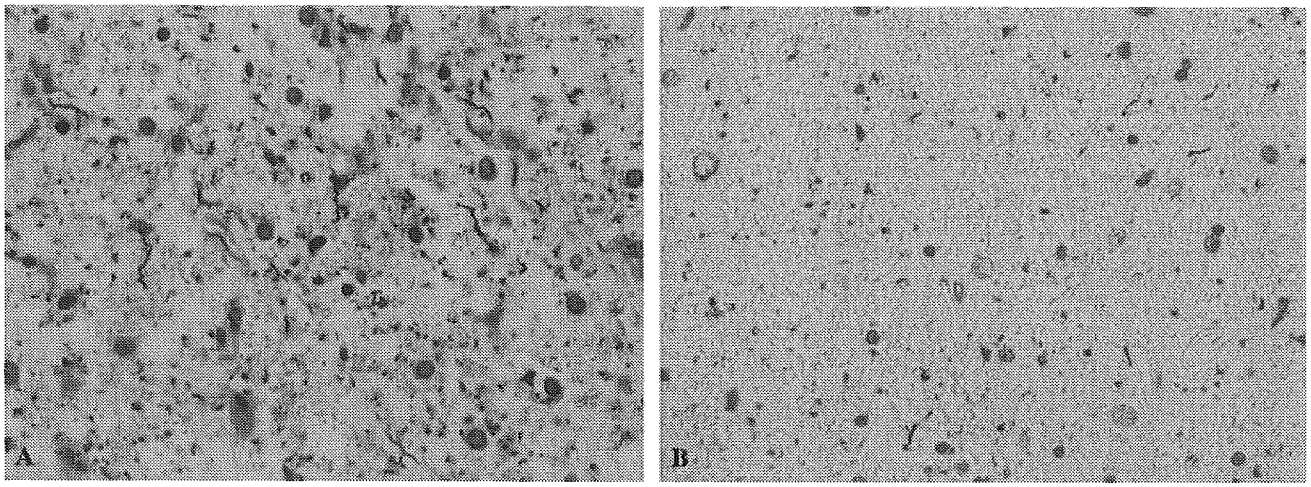

Fig. 1 White matter lesions of the CBD spinal cord. Several neuropil threads are present in marginal areas of the cervical anterior horn (**A**, patient 4, G-B stain; **B**, patient 8, AT-8 tau immunostain (*CBD* corticobasal degeneration, *G-B* Gallyas-Braak). **A**, **B** ×40

Table 2 Neuropil threads detected by Gallyas-Braak staining (+ + + numerous, + + moderate number, + several, ± a few, − none)

Patient	A. Cervical white matter			B. Cervical gray matter		
	Anterior funiculus	Lateral funiculus	Posterior funiculus	Anterior horn	Intermediate gray matter	Posterior horn
1	±	−	−	+ +	+ + +	+
2	−	−	−	+ +	+ +	+
3	±	−	−	+	+ +	+
4	+	±	−	+ +	+ + +	+ +
5	−	−	−	+	+ +	±
6	−	−	−	+	+ +	+
7	±	−	−	+	+ +	±
8	+	±	−	+	+ +	+

Table 3 Gallyas-Braak-positive neurons in cervical segments (+ + + >6 positive neurons, + + 3–6 positive neurons, + 1–3 positive neurons, ± 0–1 positive neurons, – no positive neurons)

Patient	Anterior horn	Intermediate gray matter	Posterior horn
1	±	+ +	–
2	±	+ +	±
3	±	+ +	±
4	+	+ + +	+
5	±	+ +	+
6	±	+	–
7	±	+ +	±
8	+	+ +	–

cervical gray matter in Tables 2B and 3, respectively). Widespread neuropil threads were observed in the gray matter, and the density of neuropil threads varied between patients, but the pattern was relatively uniform and prominent in the intermediate gray matter (Fig. 2A–H). In the intermediate gray matter, although neuropil threads were frequently observed in the medial, lateral, and reticular portions, there were only a few neuropil threads in the intermediolateral column and Clarke's column. In the anterior horn of cervical segments, neuropil threads were prominent in the medial division, and their density decreased laterally toward the lateral division. Several G-B- or AT-8-tau-positive neuronal inclusions were identified, predominantly in the intermediate gray matter, and a few were identified in the anterior and posterior horns (Fig. 3A, B). Very few neuronal inclusions were identified in the intermediolateral column or Clarke's column. There were a few large motor neurons positive for G-B staining or AT-8 tau immunostaining. Neuronal inclusions were of the globose type (Fig. 4A), suggestive of NFTs, or showed diffuse granular accumulation of cytoplasmic tau (Fig. 4B), suggestive of pretangles. No typical NFTs, as identified by Bodian silver staining, were identified in any CBD patient. The number of neuropil threads in

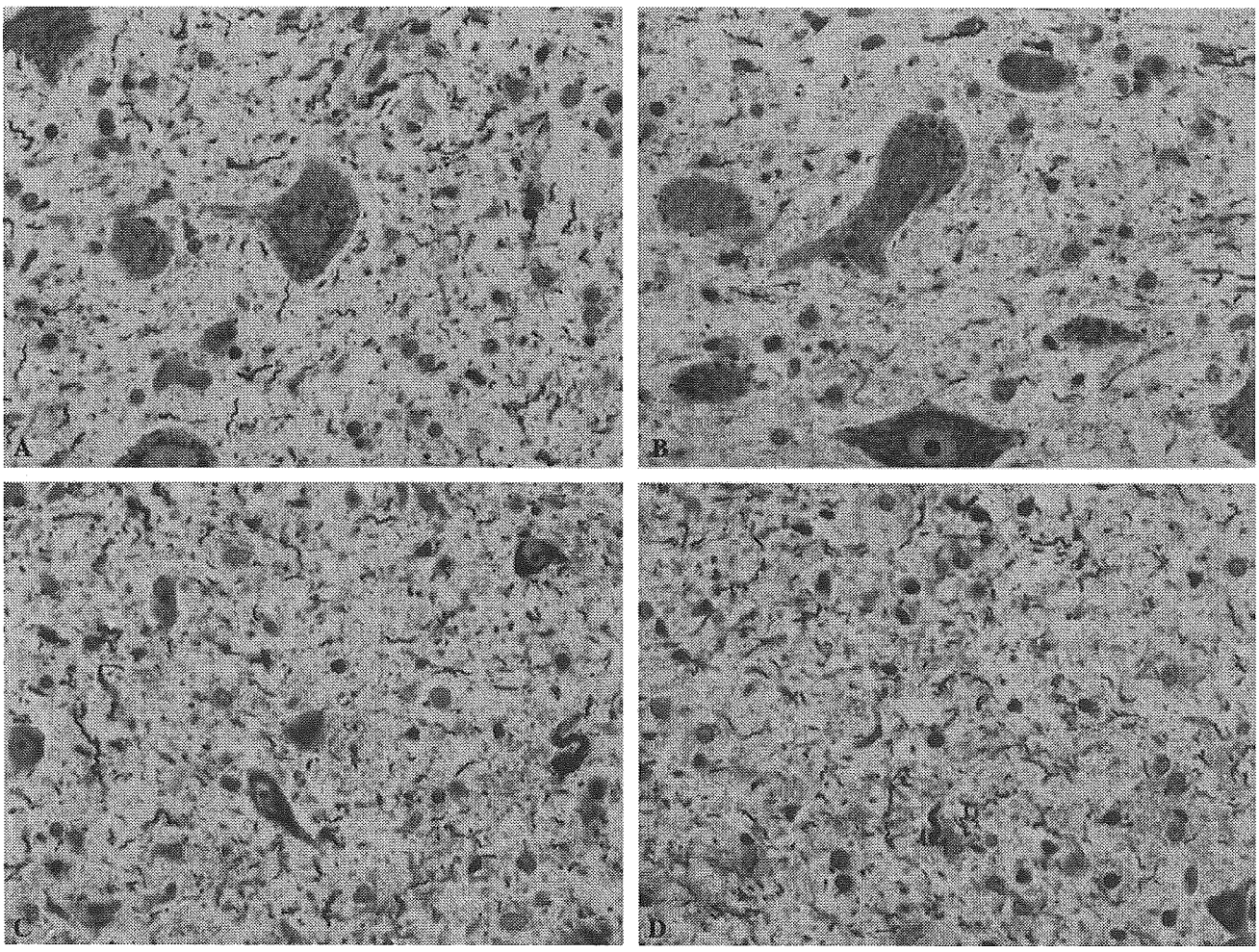

Fig. 2 Representative gray matter lesions of a CBD spinal cord (patient 4, G-B stain). **A** Medial division of the anterior horn in a cervical segment, **B** lateral division of the anterior horn in a cervical segment, **C** medial portion of the intermediate gray matter in a cervical segment, **D** lateral portion of the intermediate gray matter in a cervical segment, **E** intermediolateral column in an upper thoracic segment, **F** Clarke's column in an upper thoracic segment, **G** basal portion of posterior horn in a cervical segment, **H** substantia gelatinosa of the posterior horn in a cervical segment. **A–H** ×40

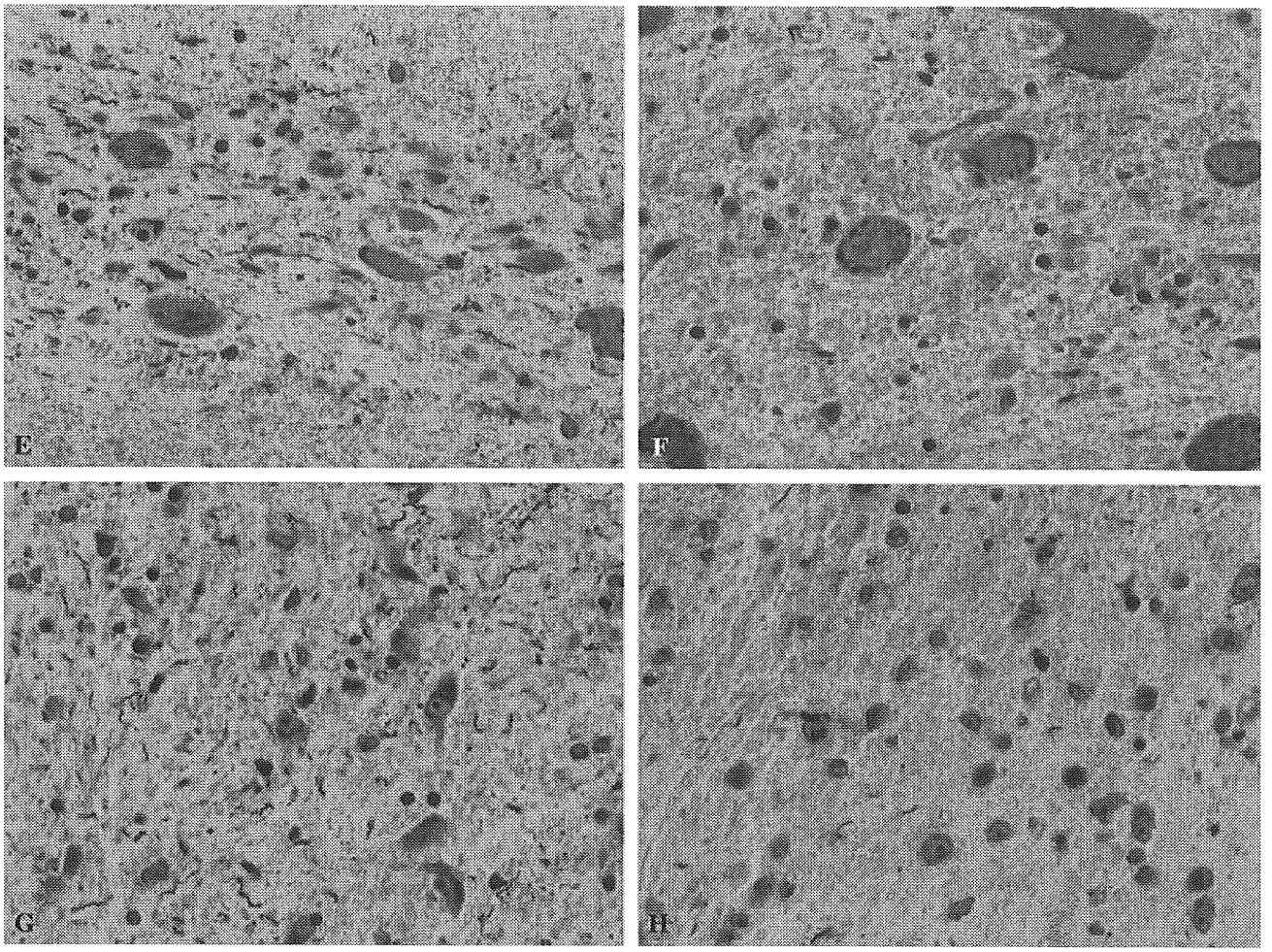

Fig. 2 (Contd.)

each case correlated well with the number of neurons positive for G-B staining or AT-8 tau immunostaining. The distribution pattern and density of neuropil threads and G-B- or AT-8-tau-positive small neurons were similar to the distribution pattern and density of interneurons and their processes, particularly in cervical segments. Neuropil threads and neuronal inclusions were clearly more prominent in cervical segments than in thoracolumbosacral segments, and they decreased in density caudally.

The density of neuropil threads and neuronal inclusions in the CBD spinal cords appeared not to correlate with age at death or disease duration. Neuropil threads in the spinal cord were short, and many were dot-like in shape. Neuropil threads were much more abundant in the gray matter than in the white matter. Asymmetric pathological lesions of the white and gray matter were not identified in any CBD patient regardless of the presence of asymmetric signs. No typical astrocytic plaques were present in any CBD spinal cord. Coiled bodies were noted in the white and gray matter but were not quantified because there were so few. No tau-positive or argyrophilic structures were identified in any control spinal cord.

Discussion

The spinal cord lesions of CBD have seldom been described, and rarely in detail [8, 11, 13, 18]. In the original report by Rebeiz et al. [13], the lesions of two spinal cords were briefly described. In one case, no abnormalities were found, and in another, a few anterior horn cells showed swelling and central chromatolysis, typical of an axonal reaction, but the posterior column in each case appeared normal [13]. Mori et al. [11] described two cases of CBD with widespread abnormal tau and NFTs, and reported the presence of tau-positive neurons and argyrophilic inclusions, no neuronal loss, and no astrocytosis in the spinal cord. Wakabayashi et al. [18] reported three cases of CBD in which they observed tau immunoreactivity in the cytoplasm of a few cells in the spinal cord gray matter. Kikuchi et al. [8] observed preferential neurodegeneration in the cervical spinal cord in progressive supranuclear palsy using microtubule-associated protein 2 (MAP2) immunostaining; MAP2 immunoreactivity was almost completely preserved in the gray matter in each of two CBD spinal cords, and neither NFTs nor GFTs were detected.

In the present study, we examined the spinal cord lesions of eight CBD patients, paying particular atten-

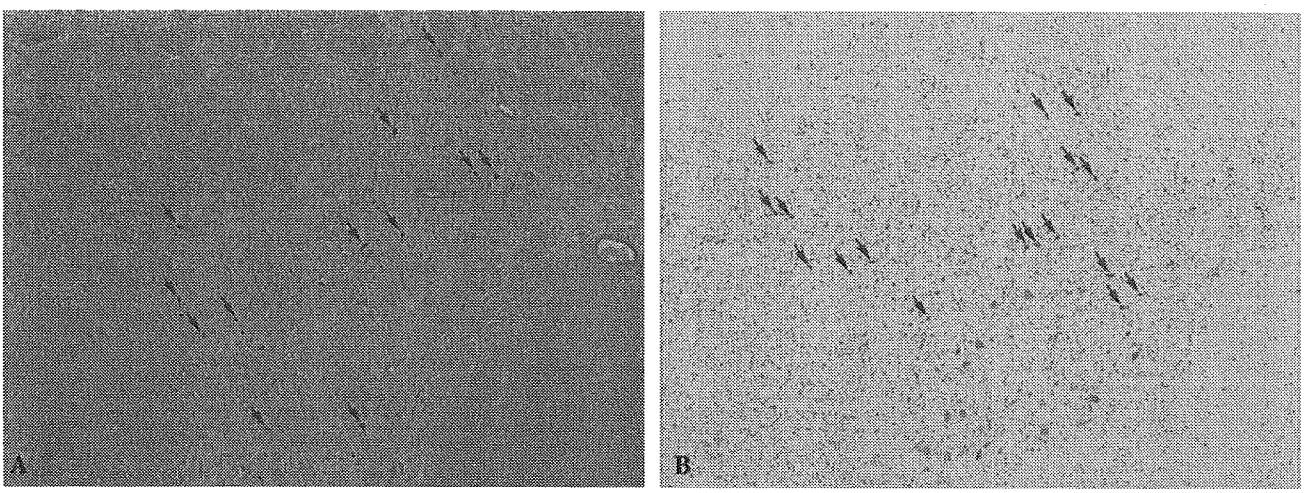

Fig. 3 Identification of G-B- or AT-8 tau-positive neuronal inclusions. Several G-B- or AT-8 tau-positive neuronal inclusions are identified predominantly in the intermediate gray matter (*arrow*), and a few are identified in the anterior and posterior horns (**A** patient 4, G-B stain; **B** patient 8, AT-8 tau immunostain; cervical segment). **A**, **B** ×4

tion to the presence of tau-positive and argyrophilic structures; some findings were notable, including white and gray matter lesions. We believe the most important finding of the present study is the identification of widespread neuropil threads and many neuronal inclusions in the CBD spinal cord, particularly in the cervical intermediate gray matter. Because no tau-positive or argyrophilic structures were identified in the five control patients, our results indicate that CBD involves an abnormal tau-degenerative alteration in the spinal cord. The density of neuropil threads and neuronal inclusions did not appear to correlate with age or disease duration. For example, patient 4, with disease of 4-year duration and death at age of 68, showed the most numerous neuropil threads and neuronal inclusions; patient 6, with disease of 4-year duration and death at age 69, showed the fewest such structures.

With regard to GFTs, although some authors have argued that astrocytic plaques are characteristic of CBD [5, 6, 11, 15], astrocytic plaques were not identified in any CBD spinal cord in the present study. Whereas the CBD spinal cords showed extensively positive G-B-stained and AT-8 tau-immunostained neurons, Bodian silver staining was not present in any CBD spinal neurons. These neurons comprised mostly small neurons and may have been pretangles [7]. Although neurons positive for AT-8 tau immunostaining do not necessarily show NFTs in cases of CBD, diffusely stained tau-positive substance may constitute an early NFT change [11]. The majority of tau-positive neurons in CBD interact with fibrillary structures such as NFTs, suggesting that the fibrillary conformation of tau is not prominent in CBD [17]. Tau-positive neurons in CBD do not form the fibrillary structures observed in Alzheimer's disease; they remain mostly in the nonfibrillary state without the development of typical NFTs [16].

Small neurons in the intermediate gray matter of the spinal cord are thought to comprise mainly interneurons

Fig. 4 Representative neuronal inclusions. **A** Globose-type neuronal inclusion in the intermediate gray matter (patient 7, cervical segment, G-B stain). **B** Pretangle-like neuronal inclusion in the intermediate gray matter (patient 4, cervical segment, AT-8 tau immunostain). **A**, **B** ×100

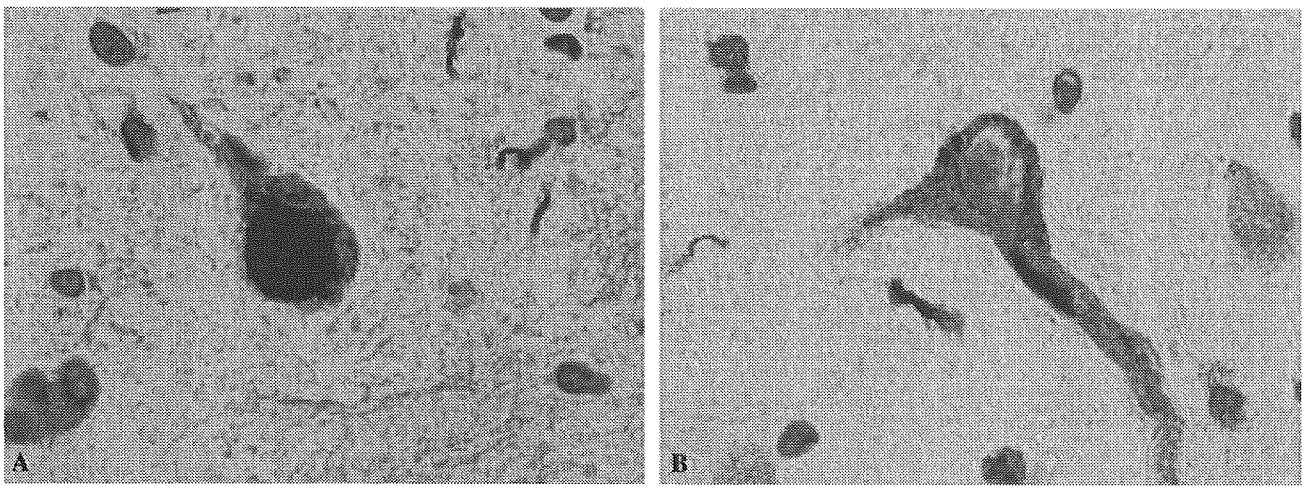

[9]. It is noteworthy that the distribution of neuropil threads and small neurons positive for G-B staining and AT-8 tau immunostaining was similar to that of interneurons and their processes, particularly in cervical segments. Activity of the descending fibers of the extrapyramidal system, such as those of the rubrospinal tract, reticulospinal tract, and medial longitudinal fasciculus, is mediated by interneurons in the cervical segments [9]. These interneurons are thought to be involved in focal dystonia such as nuchal dystonia [8, 9]. In the present study, spinal white matter lesions did not correlate with spinal gray matter lesions, implying that the white matter lesions do not necessarily cause the gray matter lesions. We believe that the gray matter lesions represent not only secondary degeneration due to the white matter lesions but also a primary degenerative response in the CBD pathological process. We also believe that the presence of neuropil threads and neuronal inclusions in the intermediate gray matter, particularly in cervical segments, may be part of the cause of the axial or nuchal rigidity of CBD. However, in the present study no asymmetric lesions of the spinal cord in the white or gray matter were identified in patients with or without clinical asymmetric motor dysfunction. Because clinical signs may result from widespread pathological involvement of the cerebral cortex [5, 6], basal ganglia, or brainstem, evaluation of the relation between clinical signs and pathological spinal cord changes may be difficult.

Although further studies are necessary to elucidate the underlying pathological mechanisms of CBD spinal cord lesions, it is clear that the widespread presence of neuropil threads and neuronal inclusions, particularly in cervical segments, is an important pathological feature of CBD. These findings suggest that the spinal cord, in addition to the cerebrum and brainstem, is involved in the pathological process of CBD.

References

1. Braak H, Braak E, Ohm T, Bohl J (1988) Silver impregnation of Alzheimer's neurofibrillary changes counterstained for basophilic material and lipofuscin pigment. Stain Technol 63:197–200
2. Dickson DW, Bergeron C, Chin SS, Duyckaerts C, Horoupian D, Ikeda K, Jellinger K, Lantos PL, Lippa CF, Mirra SS, Tabaton M, Vonsattel JP, Wakabayashi K, Litvan I (2002) Office of Rare Diseases neuropathologic criteria for corticobasal degeneration. J Neuropathol Exp Neurol 61:935–946
3. Fahn S (1995) Parkinsonism. In: Rowland LP (ed) Merritt's textbook of neurology, 9th edn. Williams & Wilkins, Baltimore, pp 713–730
4. Gibb WR, Luthert PJ, Marsden CD (1989) Corticobasal degeneration. Brain 112:1171–1192
5. Hattori M, Hashizume Y, Yoshida M, Iwasaki Y, Hishikawa N, Ueda R, Ojika K (2003) Distribution of astrocytic plaques in the corticobasal degeneration brain and comparison with tuft-shaped astrocytes in the progressive supranuclear palsy brain. Acta Neuropathol 106:143–149
6. Iwasaki Y, Yoshida M, Hattori M, Goto A, Aiba I, Hashizume Y, Sobue G (2004) Distribution of tuft-shaped astrocytes in the cerebral cortex in progressive supranuclear palsy. Acta Neuropathol 108:399–405
7. Iwatsubo T, Hasegawa M, Ihara Y (1994) Neuronal and glial tau-positive inclusions in diverse neurologic diseases share common phosphorylation characteristic. Acta Neuropathol 88:129–136
8. Kikuchi H, Doh-ura K, Kira J, Iwaki T (1999) Preferential neurodegeneration in the cervical spinal cord of progressive supranuclear palsy. Acta Neuropathol 97:577–584
9. Kuypers HG (1982) A new look at the organization of the motor system. Prog Brain Res 57:381–403
10. Litvan I, Agid Y, Goetz C, Jankovic J, Wenning GK, Brandel JP, Lai EC,Verny M, Ray-Chaudhuri K, Mckee A, Jellinger K, Pearce RK, Bartko JJ (1997) Accuracy of the clinical diagnosis of corticobasal degeneration: a clinicopathologic study. Neurology 48:119–125
11. Mori H, Nishimura M, Namba Y, Oda M (1994) Corticobasal degeneration: a disease with widespread appearance of abnormal tau and neurofibrillary tangles, and its relation to progressive supranuclear palsy. Acta Neuropathol 88:113–121
12. Paulus W, Seli M (1990) Corticonigral degeneration with neuronal achromasia and basal neurofibrillary tangles. Acta Neuropathol 81:89–94
13. Rebeiz JJ, Kolodny EH, Richardson EP Jr (1968) Corticodentatonigral degeneration with neuronal achromasia. Arch Neurol 18:20–33
14. Riley DE, Lang AE, Lewis A, Resch L, Ashby P, Hornykiewicz O, Black S (1990) Cortical-basal ganglionic degeneration. Neurology 40:1203–1212
15. Tsuchiya K, Ikeda K, Uchihara T, Oda T, Shimada H (1997) Distribution of cerebral cortical lesions in corticobasal degeneration: a clinicopathological study of five autopsy cases in Japan. Acta Neuropathol 94:416–424
16. Uchihara T, Nakamura A, Yamazaki M, Mori O (2001) Evolution from pretangle neurons to neurofibrillary tangles monitored by thiazin red combined with Gallyas method and double immunofluorescence. Acta Neuropathol 101:535–539
17. Uchihara T, Nakamura A, Yamazaki M, Mori O, Ikeda K, Tsuchiya K (2001) Different conformation of neuronal tau deposits distinguished by double immunofluorescence with AT8 and thiazine red combined with Gallyas method. Acta Neuropathol 102:462–466
18. Wakabayashi K, Oyanagi K, Makifuchi T, Ikuta F, Homma A, Homma Y, Horikawa Y, Tokiguchi S (1994) Corticobasal degeneration: etiopathological significance of the cytoskeletal alterations. Acta Neuropathol 87:545–553

Gene Expression Profile of Spinal Motor Neurons in Sporadic Amyotrophic Lateral Sclerosis

Yue-Mei Jiang, PhD,[1] Masahiko Yamamoto, MD,[1] Yasushi Kobayashi, MD,[1] Tsuyoshi Yoshihara, PhD,[1] Yideng Liang, PhD,[1] Shinichi Terao, MD,[2] Hideyuki Takeuchi, MD,[1] Shinsuke Ishigaki, MD,[1] Masahisa Katsuno, MD,[1] Hiroaki Adachi, MD,[1] Jun-ichi Niwa, MD,[1] Fumiaki Tanaka, MD,[1] Manabu Doyu, MD,[1] Mari Yoshida, MD,[3] Yoshio Hashizume, MD,[3] and Gen Sobue, MD[1]

The causative pathomechanism of sporadic amyotrophic lateral sclerosis (ALS) is not clearly understood. Using microarray technology combined with laser-captured microdissection, gene expression profiles of degenerating spinal motor neurons isolated from autopsied patients with sporadic ALS were examined. Gene expression was quantitatively assessed by real-time reverse transcription polymerase chain reaction and in situ hybridization. Spinal motor neurons showed a distinct gene expression profile from the whole spinal ventral horn. Three percent of genes examined were downregulated, and 1% were upregulated in motor neurons. Downregulated genes included those associated with cytoskeleton/axonal transport, transcription, and cell surface antigens/receptors, such as dynactin, microtubule-associated proteins, and early growth response 3 (EGR3). In contrast, cell death–associated genes were mostly upregulated. Promoters for cell death pathway, death receptor 5, cyclins A1 and C, and caspases-1, -3, and -9, were upregulated, whereas cell death inhibitors, acetyl-CoA transporter, and NF-κB were also upregulated. Moreover, neuroprotective neurotrophic factors such as ciliary neurotrophic factor (CNTF), Hepatocyte growth factor (HGF), and glial cell line–derived neurotrophic factor were upregulated. Inflammation-related genes, such as those belonging to the cytokine family, were not, however, significantly upregulated in either motor neurons or ventral horns. The motor neuron–specific gene expression profile in sporadic ALS can provide direct information on the genes leading to neurodegeneration and neuronal death and are helpful for developing new therapeutic strategies.

Ann Neurol 2005;57:236–251

Amyotrophic lateral sclerosis (ALS) is a devastating neurodegenerative disease characterized by loss of motor neurons in the spinal cord, brainstem, and motor cortex.[1] Initial symptoms include weakness of the limbs, abnormalities of speech, and difficulties in swallowing. The weakness ultimately progresses to complete paralysis, and half of the patients die within 3 years after the onset of symptoms, mostly because of respiratory failure. Approximately 10% of all ALS patients show familial traits, and 20 to 30% of familial ALS patients are associated with a mutation in the copper/zinc superoxide dismutase 1 gene (SOD1). However, more than 90% of ALS patients are sporadic, not showing any familial trait. The presence of Bunina bodies in the remaining spinal motor neurons is a hallmark of sporadic ALS cases.[2,3] So far, several hypotheses about the pathogenesis of sporadic ALS have been proposed based on extensive research on sporadic ALS: oxidative stress, glutamate excitotoxicity, impaired axonal transport, mitochondrial dysfunction, neurotrophic deprivation, proteasomal dysfunction, neuroinflammation, autoimmunity, viral infection, and others.[4–11] Nevertheless, the actual pathogenic mechanism of the selective motor neuron degeneration and ultimate cell death in sporadic ALS remains unknown. There have been extensive studies using animal models and culture systems for familial ALS, especially with SOD1 mutations, but no similar approach is available for studying sporadic ALS.

Recently advances in DNA microarray technology make it possible to analyze global gene expression profiles of thousands of genes in normal as well as pathological tissues. Global gene expression studies using DNA microarray technology have generated valuable

From the [1]Department of Neurology, Nagoya University Graduate School of Medicine, Nagoya; [2]Department of Internal Medicine, Aichi Medical University School of Medicine; and [3]Department of Neuropathology, Institute for Medical Science of Aging, Aichi Medical University School of Medicine, Nagakute, Aichi, Japan.

Received Sep 7, 2004, and in revised form Oct 22. Accepted for publication Nov 14, 2004.

Published online Jan 26, 2005, in Wiley InterScience (www.interscience.wiley.com). DOI: 10.1002/ana.20379

Address correspondence to Dr Sobue, Department of Neurology, Nagoya University Graduate School of Medicine, Nagoya 466-8550, Japan. E-mail: sobueg@med.nagoya-u.ac.jp

information about cell behavior in tissues consisting of homogeneous cell types, cultured cells, and cancer tissues of monoclonal origin.[12,13] In the case of neuronal tissues, particularly those of patients with neurological diseases, however, the complexity of tissues containing multiple lineages of cells, such as neurons, glial cells, and vascular tissues, places limitations on the use of DNA microarray technology. In the lesions of ALS spinal cords, there are reduced numbers of motor neurons with glial cell proliferation, making it difficult to examine motor neuron–specific gene expression.

Laser-captured microdissection (LCM) has been reported to make it possible to isolate single individual neurons from neural tissues with well-preserved mRNA quality.[14,15] In addition, RNA amplification techniques preserving the relative amounts of individual mRNAs have been developed recently.[16,17] LCM and RNA amplification combined with DNA microarray analyses have been reported to enable studies of cell type–specific gene expression profiles in tissues with multiple cell lineages.[16,18] Such integrated analysis system provide an effective tool for investigating the cellular events affecting cell type–specific gene expression profiles in neurodegenerative diseases such as ALS. Indeed, we and other groups demonstrated that these integrated systems could be applied successfully to describe cell-specific gene expression profiles in neuronal tissues.[15,18]

In this study, we applied integrated LCM, RNA amplification, and DNA microarray analysis to clarify alterations of motor neuron–specific gene expression in sporadic ALS cases and successfully obtained expression gene database in situ from degenerating motor neurons in sporadic ALS spinal cord.

Patients and Methods

Tissues from Amyotrophic Lateral Sclerosis and Control Patients

Fresh specimens of lumbar spinal cord (L4 to L5 segment) from 14 sporadic ALS patients (nine men, five women) and 13 neurologically normal patients (nine men, four women) were obtained at autopsy (Table 1). Diagnosis of ALS was

Table 1. Details of Patients Examined in This Study

Patients	Sex	Age (yr)	Duration of Illness (yr)	Postmortem Delay (hr)	Diseases	Spinal Cord Neuropathology Motor Neuron Loss/Gliosis
ALS1	M	72	3.7	6	ALS (B, UL, LL)	Moderate/mild
ALS2	M	71	2.3	5	ALS (LL, UL)	Moderate/mild
ALS3	M	58	1.8	13	ALS (UL, LL, B)	Severe/severe
ALS4	M	43	2.6	5	ALS (LL, B)	Moderate/mild
ALS5	M	53	2.8	11	ALS (B, UL, LL)	Moderate/severe
ALS6	F	79	4.0	4	ALS (UL, LL, B)	Severe/severe
ALS7	F	59	2.5	3	ALS (UL)	Mild/mild
ALS8	F	67	2.0	7	ALS (UL, B)	Severe/mild
ALS9	M	74	4.3	10	ALS (LL, B)	Severe/mild
ALS10	F	47	1.8	4	ALS (B, UL, LL)	Mild/mild
ALS11	M	74	4.5	12	ALS (UL, LL)	Moderate/mild
ALS12	M	57	3.5	5	ALS (LL, UL)	Severe/mild
ALS13	F	53	3.0	8	ALS (B, UL, LL)	Severe/severe
ALS14	M	63	2.2	5	ALS (UL, B)	Mild/mild
Control1	M	57	—	7	Pneumonia	No
Control2	M	78	—	10	Cerebral infarction	No
Control3	M	72	—	9	Lung cancer	No
Control4	F	52	—	7	Pneumonia	No
Control5	F	65	—	12	Pneumonia	No
Control6	M	75	—	10	Heart failure	No
Control7	M	42	—	5	Heart failure	No
Control8	F	76	—	5	Pancreas cancer	No
Control9	F	84	—	6	Myocardial infarction	No
Control10	M	48	—	13	Heart failure	No
Control11	M	77	—	11	Heart failure	No
Control12	M	66	—	11	Cerebral infarction	No
Control13	M	75	—	4	Pneumonia	No

The age, duration of illness, and postmortem delay are indicated for the ALS and control cases. Predominant clinical features of ALS are shown: UL = upper limbs; LL = lower limbs; B = bulbar. Neuropathological involvement of spinal cords was graded as previously. Ten ALS samples were used for microarray analysis: five of them (1, 7, 10, 11, and 14) were analyzed using 4.8K array for spinal motor neurons; five (2, 4, 5, 8, and 12) using 1.0K for spinal motor neurons; five (1, 3, 10, 13, and 14) using 4.8K for spinal ventral horn gray matter; and five (1, 2, 4, 5, and 13) and five (1, 2, 7, 8, and 10) control samples using 4.8K and 1.0K. Thirteen ALS (1–13) and 11 (1–11) control samples were used for TaqMan reverse transcription polymerase chain reaction analysis. Five ALS (1, 10, 11, 13, and 14) and four control (1, 3, 5, and 12) samples were used for in situ hybridization and immunohistochemistry.
ALS = amyotrophic lateral sclerosis.

confirmed by El Escorial diagnostic criteria defined by the World Federation of Neurology and the histopathological findings, particularly the presence of the Bunina body.[2,3] All cases of ALS were sporadic and did not show any heredity. ALS patients with *SOD1* mutation were excluded. The collection of tissues and their use for this study were approved by the ethics committee of Nagoya University Graduate School of Medicine. Tissues were frozen immediately and stored at −80°C until use. The mean ages and standard deviations for ALS and control patients were 62.1 ± 11.0 and 66.7 ± 13.1 years, and the mean postmortem intervals and standard deviations were 7.0 ± 3.3 and 8.5 ± 3.0 hours, respectively. The differences between the means of either age or postmortem interval were not significant between the ALS and control groups. The cause of death in all ALS patients was respiratory failure, and the causes in the control patients were pneumonia, lung cancer, or acute heart failure (see Table 1). Parts of the lumbar spinal cord were fixed in 10% buffered formalin solution, and processed for paraffin sections. The sections were stained with hematoxylin and eosin and Klüver-Barrera and Holzer techniques, and histological assessment was performed. The degree of motor neuron loss and astrogliosis was ranked as mild, moderate or severe according to previously reported.[19,20]

Laser-Captured Microdissection of Spinal Motor Neurons

Sections (10μm) were cut with a standard cryostat, mounted on poly-L-lysin coated slides (Zeiss, Thornwood, NY), and stained with hematoxylin to identify the motor neurons located in the medial and lateral nuclei of the ventral horns of lumber spinal cords. After staining with hematoxylin, the sections were washed in RNase-free water and dried.[21,22] The PALM Robot-Microbeam system (P.A.L.M. Mikrolaser Technology AG, Bernried, Germany) was used for laser capture. The pulsed laser microbeam cut precisely around the targeted motor neurons in the spinal ventral horn (LCM; see Fig 1A–C). The identity of motor neurons was ascertained by reverse transcription polymerase chain reaction (RT-PCR) for choline acetyltransferase (ChAT) as described previously.[15] Each laser-isolated specimen subsequently was ejected from the glass slide with a single or several laser shots and collected directly into the cap of a PCR tube containing denaturing buffer by a process of laser pressure catapulting in the totally noncontact manner previously described.[23] The LCM-isolated cells (approximately 500 pooled cells) were dissolved in denaturing buffer (StrataPrep Total RNA Microprep Kit; Stratagene, San Diego, CA) and stored at −80°C until use.

RNA Extraction of Laser-Captured Microdissection Motor Neuron Samples and Spinal Ventral Horn Homogenates

LCM-isolated cells in denaturing buffer were thawed and centrifuged briefly before the RNA was extracted using a StrataPrep Total RNA Microprep Kit (Stratagene) according to the manufacturer's protocol. RNA was extracted as well from the total homogenates of ventral horn gray matter of spinal cords,[19] which was dissected under a dissecting microscope.

Reverse Transcription and T7 RNA Polymerase Amplification of RNA

Ten microliters of purified RNA obtained as described above was mixed with 1μl of 0.5μg/ml T7-oligodT primer (5′-TCTAGTCGACGGCCAGTGAATTGTAATACGACTCACTATAGGGCGT$_{21}$-3′) to initiate first-strand synthesis. The primer and RNA were incubated in 4μl of 5 × first-strand reaction buffer, 0.1M DTT (2μl), 10mM dNTPs (1μl), 1μl of RNasin, and 1μl of Superscript II reverse transcriptase (Invitrogen, Carlsbad, CA) at 42°C for 1 hour, and then 30μl of 5 × second-strand synthesis buffer, 10mM dNTPs (3μl), 4μl of DNA polymerase, 1μl of *Escherichia coli* RNase H, and 1μl of *E. coli* DNA ligase and 91μl of RNase-free H_2O were added, and the mixture was incubated at 16°C for 2 hours and then at 16°C for 10 minutes after the addition of 2μl of T4 DNA polymerase. Next, an Ampliscribe T7 Transcription Kit (Epicentre Technologies, Madison, WI) was used for RNA amplification: 8μl double-stranded cDNA, 2μl of 10 × Ampliscribe T7 buffer, 1.5μl each of 100mM ATP, CTP, GTP, and UTP, 0.1 M DTT (2μl), and 2μl of T7 RNA polymerase were incubated at 42°C for 3 hours.

For second-round amplification, 10μl of amplified RNA (aRNA) from first-round amplification was mixed together with 1μl of 1mg/ml random hexamers (Invitrogen), and then first-stranded cDNA was synthesized, followed by second-stranded cDNA synthesis as described above. The double-stranded cDNA was subjected to second-round T7 in vitro transcription as above and then subsequent third-round aRNA amplification. After third-round amplification, aRNA was treated with DNase (Wako, Kanagawa, Japan) and cleaned up using an RNeasy Kit (Qiagen, Valencia, CA) according to the manufacturer's protocol.

DNA Microarray Analysis

Fluorescent cDNA probes were synthesized from aRNA of laser-captured spinal motor neurons and RNA from ventral spinal tissue homogenates using an Atlas Glass Fluorescent Labeling Kit (Clontech, Palo Alto, CA) according to the manufacturer's protocol. Cy3-labeled cDNA probes were synthesized from ALS samples for spinal motor neurons and homogenates, and Cy5-labeled cDNA probes were synthesized from control samples. BD Atlas Glass Microarray Human 1.0 and 3.8 (Clontech) slides were hybridized with these fluorescent labeled probes overnight at 50°C and then washed four times and dried according to the manufacturer's protocol. Individual Cy3-labeled cDNA probes from ALS RNA samples of spinal motor neurons and homogenates for each patient were coupled with Cy5-labeled cDNA probes from control RNA samples of those tissues, which were prepared by mixing equal amounts of RNA samples amplified from the control patients. The microarrays were scanned in a laser scanner (GenePix 4000; Axon Instruments, Union City, CA), and the resulting signals were quantified and stored using GenePix Pro analysis software (Axon Instruments). The data for each expressed gene obtained from microarray analysis were expressed as the ratios of the values of individual ALS patients or the means of the values of ALS to the values of the control patients. The values of gene expression levels were means-calculated from motor neurons of 5 or 10 inde-

pendent individuals with ALS as well as from spinal ventral horns of 5 individuals with ALS.

Quantitative Real-Time Reverse Transcription Polymerase Chain Reaction

The probe and primers for the real-time PCR were designed using Primer3′ (S. Rozen and H. J. Skaletsky, available at http://www-genome.wi.mit.edu/genome_software/other/primer3.html). TaqMan PCR was conducted using an iCycler system (Bio-Rad Laboratories, Hercules, CA) with a QuantiTect Probe PCR Kit (Qiagen) and the cDNA according to the manufacturer's protocol. The reaction conditions were 95°C for 3 minutes and then 50 cycles of 15 seconds at 95°C followed by 60 seconds at 55°C. All experiments were performed in quadruplicate, and several negative controls were included. For an internal standard control, the expression of glyceraldehyde-3-phosphate dehydrogenase (GAPDH) was simultaneously quantified. The primers and probe sequences for the examined genes (acetyl-CoA transporter: D88152; Bak: NM_001188; CRABP1: NM_004378; cyclin C: M74091; dynactin 1: NM_004082; EGR3: NM_004430; ephrin A1: M57730; GAPDH: NM_002046; KIAA0231: D86984; and TrkC: U05012) were described in the legends for Figure 3. The threshold cycles of each gene were determined as the number of PCR cycles at which the increase in reporter fluorescence reached 10 times above the baseline signal. The weight ratio of the target gene to GAPDH gives the standardized expression level.

In Situ Hybridization

Frozen sections (10μm thick) of the spinal cord were prepared and immediately fixed in 4% paraformaldehyde. Then, they were treated with 0.1% diethylpyrocarbonate (DEPC) twice for 15 minutes and prehybridized at 45°C for 1 hour. Digoxigenin-labeled cRNA probes were generated from linearized plasmids for the genes of interest using SP6 or T7 polymerase (Roche Diagnostics, Basel, Switzerland). Gene names, Genebank accession number, probe position (nucleotide number), and probe size were as follows: acetyl-CoA transporter, D88152, nucleotides 397-741, 345bp; Bak, NM_001188, nucleotides 792–2094, 345bp; CRABP1, NM_004378, nucleotides 210–545, 336bp; dynactin 1, NM_004082, nucleotides 2392–2774, 383bp; DR5, NM_004082, nucleotides 682–1070, 389bp; EGR3, NM_004430, nucleotides 1433–1794, 362bp; KIAA0231, D86984, nucleotides 698–1053, 356bp; TrkC, U05012, nucleotides 1412–1721, 310bp. After prehybridization, the sections were hybridized with each digoxigenin-labeled cRNA probe overnight at 45°C. The washed sections were incubated with alkaline phosphatase-conjugated anti–digoxigenin antibody (Roche Diagnostics). The signal was visualized with NBT/BCIP (Roche Diagnostics).

Immunohistochemistry

Frozen sections (10μm thick) of the spinal cord were prepared and immediately fixed in 4% paraformaldehyde. Then, they were blocked with 2% bovine serum albumin (Sigma) in Tris-buffered saline at room temperature for 20 minutes and incubated with anti–cyclin C (1:200 dilution; Santa Cruz Biotechnology, Santa Cruz, CA) antibody overnight at 4°C. Subsequent procedures were performed using ENVISION++KIT/HRP (diaminobenzidine tetrahydrochloride; DAKO, Carpinteria, CA) according to the manufacturer's protocol.

Statistical Analyses

To assess the correlation of intensity values for each labeling sample, we used scatterplots and measured linear relationships. The correlation coefficient, R^2, that was calculated indicates the variability of intensity values between Cy-5– and Cy-3–labeled samples. To perform cluster analyses of hierarchical clustering, self-organizing maps (SOM) and principal component analysis after logarithmic transformation, we used Acuity 3.0 software (Axon Instruments). The data measured by quantitative real-time RT-PCR analysis were analyzed by Student's t tests.

Results

T7 Amplification Preserves Gene Expression Profiles

Because the amounts of laser-microdissected samples were extremely low and did not contain enough mRNA for further analysis, RNA amplification was required. It was critical to achieve sufficient RNA amplification and yet maintain the expression profiles of mRNAs. We performed experiments to determine how the expression profiles of mRNAs were affected by the T7 amplification procedure. RNA samples were extracted from control spinal cords and a part of RNA samples was amplified using T7 amplification. One flourescently labeled probe was synthesized from an individually amplified RNA (aRNA) or nonamplified RNA (nRNA) and was hybridized to microarrays. Independent amplification of RNA yielded quite similar expression patterns. The correlation of signal intensities between independent amplifications for the third aRNA was $R^2 = 0.9157$, $p < 0.0001$, and on the other hand, the correlation of signal intensities in nRNA was $R^2 = 0.9157$, $p < 0.0001$ (Fig 1D, E). Previous reports using similar amplification procedures as ours also have confirmed the reproducibility of T7 amplification for the preservation of RNA expression profiles.[14,15,17] In this study, the third-round amplification was performed for the LCM-isolated motor neurons, but for the spinal ventral horn homogenates a single amplification produced enough RNA for further analysis, and similar expression patterns were found between the first and third amplifications (data not shown).

Gene Expression Database of Spinal Motor Neurons and Ventral Horn Homogenates of Amyotrophic Lateral Sclerosis

aRNA samples from the motor neurons and the ventral horn homogenates from the lumbar spinal cords were subjected to microarray analysis. The differences of the gene expression levels between ALS and control sam-

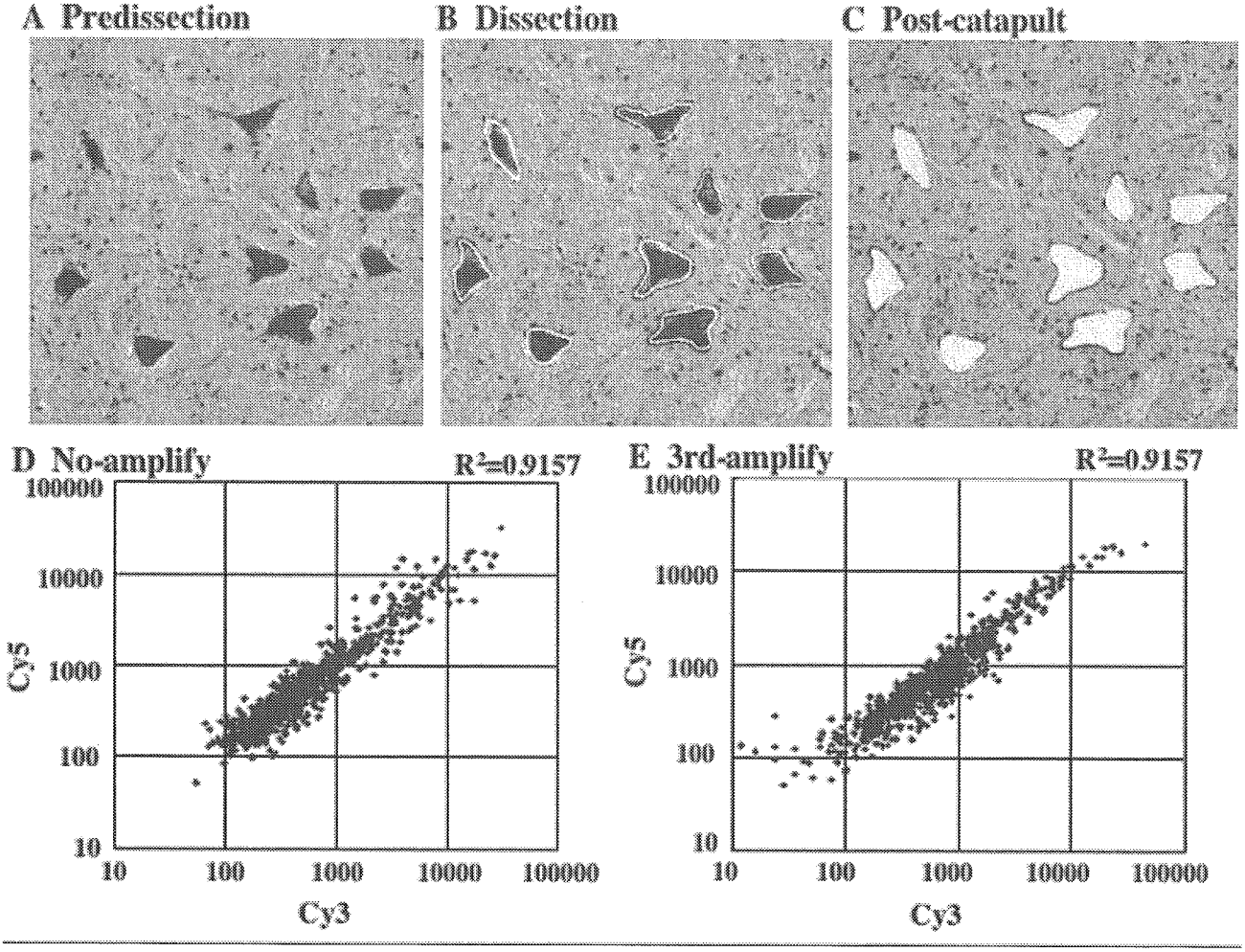

Fig 1. Verification of laser-captured microdissection (LCM) and RNA amplification. Microdissection of motor neurons in spinal ventral horn: sections were stained with hematoxylin (A); margins of motor neurons were dissected by the laser beam (B); and motor neurons were isolated from slides by laser pressure catapulting (C). Scatterplots of nonamplified and amplified RNAs: correlations between independent amplifications of control spinal cord samples are shown using nonamplified (D) and third amplified RNAs (E). These RNAs were split into two samples for labeling of Cy5 and Cy3 and hybridized separately to two microarrays. The very high squared correlations reflect the high reproducibility of the hybridization results with the same values between nonamplified and third amplified RNAs.

ples were expressed as ratios of the values of ALS individuals compared with the mean values of the controls. One percent (52/4,845) of genes examined were significantly upregulated in spinal motor neurons of ALS patients and 3% (144/4,845) were downregulated, assuming that the changes of 3.0-fold increase and 0.3-fold decrease were significant, when the mean levels of gene expression were calculated. In contrast with motor neurons, the total spinal ventral horn homogenates demonstrated 0.7% (37/4,845) and 0.2% (8/4,845) significant upregulation and downregulation of gene expression, respectively.

The genes prominently altered in ALS are listed in Tables 2 to 5 for spinal motor neurons and spinal ventral horn homogenates, respectively. Several upregulated genes listed were overlapping between spinal motor neurons (see Table 2) and ventral horns (see Table 4), suggesting that motor neuron overexpression is reflected to some extent by gene expression in ventral horn homogenates. The other genes upregulated in motor neurons were not present in the list for spinal ventral horns, because these gene expression changes were diluted and masked by changes occurring in other cell types. Because the number of spinal motor neurons was decreased in ALS spinal cords, most genes that were listed as downregulated genes in motor neurons (see Table 3) were not found in spinal ventral horns (see Table 5) except for three genes (CRABP1, EGR3, and postmeiotic segregation increased 2-like 11). When we categorized these altered genes in ALS motor neurons into several functional groups, the genes related to cell receptors and intracellular signaling, transcription,

Table 2. Upregulated Genes in ALS Motor Neurons (Top 30)

GeneBank No.	Gene Name	Fold Change (ALS/control)
NM_003419	Zinc finger protein 10 (KOX 1)	8.86
U91618	Neurotensin/neuromedin N precursor	8.33*
NM_004651	Ubiquitin-specific protease 11	8.13
D86984	KIAA0231	7.31*
A26792	Ciliary neuronotrophic factor (CNTF)	6.76
M77830	Desmoplakin I & II (DSP; DPI & DPII)	6.10
NM_005622	SA (rat hypertension-associated) homolog	5.47
NM_004733	Acetyl-coenzyme A transporter	5.33
NM_000021	Presenilin 1 (Alzheimer disease 3)	4.96
K03020	Phenylalanine-4-hydroxylase (PAH)	4.95*
AF016268	Death receptor 5 (DR5); cytotoxic TRAIL receptor, TNFR10b	4.91*
M74091	G1/S-specific cyclin C (CCNC)	4.82*
NM_000275	Oculocutaneous albinism II	4.78
AF000936	SH3-binding protein 2	4.73*
NM_000384	Apolipoprotein B	4.70
M63099	Interleukin-1 receptor antagonist	4.66*
M57730	Ephrin-A1	4.57*
L19067	NF-κ B transcription factor p65 subunit	4.52*
U66838	Cyclin A1 (CCNA1)	4.51*
NM_005021	Ectonucleotide pyrophosphatase/phosphodiesterase 3	4.48
NM_001550	Interferon-related developmental regulator 1	4.45
L25851	Integrin alpha E precursor (ITGAE)	4.43*
X16416	C-abl1 protooncogene	4.41
U08015	Transcription factor NF-ATc	4.40*
U44378	Mothers against dpp homolog 4 (SMAD4)	4.35*
NM_005067	Seven in absentia (Drosophila) homolog 2	4.22
J04536	Leukosialin precursor; sialophorin	4.19*
X06745	DNA polymerase alpha catalytic subunit	4.15*
U09564	Serine kinase	4.09*
U37139	β 3-endonexin	4.06*

Gene expression levels are expressed as means of fold-change, which is calculated by dividing the signals of each ALS sample by those of control samples, in the 5 or 10 (denoted by asterisk) patients with ALS.
ALS = amyotrophic lateral sclerosis.

metabolism, and cytoskeletal architecture were downregulated. The functional categories of secreted and extracellular communication proteins and cell cycle regulators were characteristically upregulated. A complete list of the differentially expressed genes is available online at http://www.med.nagoya-u.ac.jp/neurology/index.html.

Differential Gene Expression Profiles between Spinal Motor Neurons and Ventral Horn Homogenates of Amyotrophic Lateral Sclerosis

To compare the expression profile of motor neurons with that of spinal ventral horn homogenates, we performed cluster analyses. Because the patterns of gene expression from microarray analysis are impossible to discern by eye, data analysis software (Acuity 3.0 software; Axon Instruments) was used based on the dimensionality of the data: hierarchical clustering for high dimensional gene space and principal component analysis and SOM for low one. Hierarchical clustering clearly discriminated the expression profile of isolated motor neurons from that of ventral horn homogenates, showing two grouped branches of the dendrogram with a correlation coefficient of 0.446 (Fig 2A). Moreover, a principal component analysis confirmed the distinction of gene expression profiles between spinal motor neurons and ventral horns (see Fig 2B). The gene expression profile of motor neurons was clustered into a single cluster by the two clustering algorithms, which was well separated from that of spinal ventral horn gray matter, suggesting a relatively uniform degenerating process in spinal motor neurons in ALS.

Motor Neuron–Specific Gene Expression Profiles Identified by the Self-Organizing Map Analysis

To further analyze the expression pattern specific to spinal motor neurons, a SOM was produced as a nonhierarchical clustering.[24,25] The examined genes were subdivided into 25 clustered categories, and the selected genes are shown in a certain group of the SOM (see Fig 2C, Table 6). The genes contained in the clusters reflect the expression pattern in spinal motor neurons as well as that in spinal ventral horns, and these selected genes are somehow different from those in Tables 2 to 5 because of the different bases of classification. Clustering of the SOM showed motor neu-

Table 3. Downregulated Genes in ALS Motor Neurons (Bottom 30)

GeneBank No.	Gene Name	Fold Change (ALS/control)
NM_004378	Cellular retinoic acid–binding protein 1 (CRABP1)	0.12
NM_004430	Early growth response 3 (EGR3)	0.14
NM_005558	Ladinin 1	0.15
NM_003603	Arg/Abl-interacting protein ArgBP2	0.15
NM_000117	Emerin (Emery-Dreifuss muscular dystrophy)	0.15
NM_004357	CD151 antigen	0.15
X06820	Ras homolog gene family member B (RHOB)	0.15*
NM_003834	Regulator of G-protein signalling 11	0.16
NM_002960	S100 calcium-binding protein A3	0.16
NM_006289	Talin	0.16
NM_000964	Retinoic acid receptor, α	0.17
NM_002391	Midkine	0.17
M96944	Paired box protein PAX-5	0.17*
M74178	Hepatocyte growth factor–like protein	0.17*
NM_003822	Nuclear receptor subfamily 5, group A, member 2	0.17
NM_001188	BCL2-antagonist/killer 1; Bak	0.18
NM_000733	CD3E antigen, epsilon polypeptide (TiT3 complex)	0.18
NM_000408	Glycerol-3-phosphate dehydrogenase 2 (mitochondrial)	0.18
NM_000156	Guanidinoacetate *N*-methyltransferase	0.18*
M11886	Major histocompatibility complex, class I, C	0.18*
NM_003865	Homeo box (expressed in ES cells) 1	0.18
M36340	ADP-ribosylation factor 1 (ARF1)	0.18*
NM_001725	Bactericidal/permeability-increasing protein	0.18
NM_005334	Host cell factor C1 (VP16-accessory protein)	0.19
NM_004192	Acetylserotonin *O*-methyltransferase–like	0.19
NM_002684	Postmeiotic segregation increased 2–like 11	0.19
M11233	cathepsin D precursor (CTSD)	0.19*
NM_002313	Actin binding LIM protein 1	0.19
NM_002196	Insulinoma-associated 1	0.19
NM_002277	Keratin, hair, acidic, 1	0.19

Gene expression levels are expressed as means of fold-change, which is calculated by dividing the signals of each ALS sample by those of control samples, in the 5 or 10 (denoted by asterisk) patients with ALS.
ALS = amyotrophic lateral sclerosis.

ron–specific upregulated and downregulated gene expression commonly observed in five patients.

Clusters 1 (SOM1) and 6 (SOM6) contains 110 and 169 genes, respectively, that generally are downregulated in spinal motor neurons in all five cases examined, and those are known to be involved in the functional category of cell surface antigens and cell receptors, transcription, and cytoskeleton, whereas clusters 24 (SOM24) and 25 (SOM25) have 191 and 93 genes, respectively, that are predominantly upregulated in spinal motor neurons in all cases and belong to the functional category of cell signaling with extracellular communication, and cell death–associated proteins. The pattern of subcellular localization of their gene products also confirms the characteristics of the functional categories of upregulated and downregulated genes, that is, that plasma membrane and cytoskeletal proteins are more downregulated, and extracellular secreted proteins are more upregulated, in ALS motor neurons. All the genes listed in Table 3 are included in SOM1 and SOM6, whereas SOM24 and SOM25 do not contain all of the genes listed in Table 2. The former group of genes, with downregulation in motor neurons, included BCL2-antagonist/killer 1 (Bak) and TrkC receptor. Regarding genes related to transcription, early growth response 3 (EGR3), cellular retinoic acid–binding protein 1 (CRABP1), retinoic acid receptors, and Musashi 1 were included in SOM1 and SOM6 as downregulated genes. The expression of dynactin and microtubule-associated proteins (MAPs), which belong to the functional category of cytoskeleton and axonal transport, was downregulated in ALS motor neurons. On the other hand, KIAA0231 and acetylcoenzyme A transporter were classified into the upregulated genes in motor neurons of ALS. Regarding genes related to cell death, the expression of cyclins A1 and C, death receptor 5 (DR5), and interleukin-1 receptor antagonist was upregulated together with that of NF-κB, tumor necrosis factor (TNF) receptor–associated factor 6 (TRAF6), and caspase-1, -3, and -9 in SOM24 and SOM25. For genes in the category of trophic factor cell signaling with extracellular communication, CNTF, HGF, and glial cell line–derived neurotrophic factor (GDNF) were upregulated in ALS motor neurons, whereas midkine was downregulated. The expression of vascular endothelial growth factor as

Table 4. Upregulated Genes in Spinal Ventral Horns of ALS (Top 30)

GeneBank	Gene Name	Fold Change (ALS/control)
NM_000508	Fibrinogen, A α polypeptide	8.23
D86984	KIAA0231	6.09
NM_001801	Cysteine dioxygenase, type I	5.81
X02544	α-1-Acid glycoprotein 1 precursor	5.59
NM_001973	ELK4, ETS-domain protein (SRF accessory protein 1)	5.12
NM_000021	Presenilin 1 (Alzheimer disease 3)	5.00
NM_002097	General transcription factor IIIA	4.96
U08015	Transcription factor NF-ATc	4.96
M57730	Ephrin-A1	4.88
U91618	Neurotensin/neuromedin N precursor	4.79
AF000936	SH3-binding protein 2	4.50
NM_002949	Mitochondrial ribosomal protein L12	4.11
NM_002386	Melanocortin 1 receptor	4.03
NM_001991	Enhancer of zeste (Drosophila) homolog 1	3.93
NM_000947	Primase, polypeptide 2A (58kDa)	3.92
NM_000239	Lysozyme (renal amyloidosis)	3.88
NM_001550	Interferon-related developmental regulator 1	3.67
NM_004602	Staufen (Drosophila, RNA-binding protein)	3.66
NM_000063	Complement component 2	3.58
NM_004651	Ubiquitin-specific protease 11	3.54
NM_000397	Cytochrome b-245, β polypeptide	3.51
NM_002056	Glutamine-fructose-6-phosphate transaminase 1	3.41
L25851	Integrin α E precursor (ITGAE)	3.36
NM_004616	Transmembrane 4 superfamily member 3	3.21
NM_003720	Down syndrome critical region gene 2	3.18
J04536	leukosialin precursor; sialophorin	3.15
X06745	DNA polymerase alpha catalytic subunit	3.15
K03020	Phenylalanine-4-hydroxylase (PAH)	3.14
NM_001329	C-terminal binding protein 2	3.14
NM_000276	Oculocerebrorenal syndrome of Lowe	3.13

Gene expression levels are expressed as means of fold-change, which is calculated by dividing the signals of each ALS sample by those of control samples, in the five patients with ALS.
ALS = amyotrophic lateral sclerosis.

well as NT-3 was unchanged. Furthermore, the genes whose expression was altered significantly in spinal ventral horn homogenates as shown in Tables 4 and 5 showed similar alterations to some extent in the remaining motor neurons. However, the upregulated genes, such as integrin αE and sialophorin for cell adhesion, which were demonstrated to be spinal ventral horn–derived (see Table 4) as well as spinal motor neuron–derived (Table 2) genes, were not sorted out into SOM24 and SOM25, indicating that their upregulation occurred predominantly in glial cells.

Data Confirmation with Quantitative Real-Time Reverse Transcription Polymerase Chain Reaction, In Situ Hybridization, and Immunohistochemistry

To assure the validity of the gene expression levels detected by microarray analysis, we performed quantitative real-time RT-PCR analysis on some genes of interest using a TaqMan PCR system. Because LCM-isolated motor neurons did not contain enough RNA to perform real-time RT-PCR analysis, only selected genes were assessed in motor neurons, and for other genes the spinal ventral horn homogenates were used as the template for quantitative RT-PCR. When the extent of increase or decrease of gene expression levels was expressed as the ratio of the genes of interest to GAPDH, acetyl-CoA transporter and KIAA0231 were significantly increased 3.1-fold ($p < 0.001$) and 3.3-fold ($p < 0.01$) in spinal motor neurons of ALS, respectively (Fig 3). EGR3 expression decreased to 0.27-fold ($p < 0.01$) in ALS motor neurons. These mRNA alterations were also detected at comparable levels when using spinal ventral horn homogenates of ALS (acetyl-CoA transporter, 1.8-fold increase [$p < 0.005$]; KIAA0231, 2.3-fold increase [$p < 0.05$]; and EGR3, 0.41-fold decrease [$p < 0.01$]). In addition, the gene expression of Bak and TrkC was downregulated 0.53-fold ($p < 0.01$) and 0.40-fold ($p < 0.05$) in ALS, respectively. Moreover, increases of ephrin A1 and cyclin C expression were observed to the extents of 2.5-fold ($p < 0.05$) and 4.9-fold ($p < 0.01$), whereas dynactin 1 mRNA was downregulated 0.44-fold ($p < 0.01$), and CRABP1 mRNA was also downregulated to 0.59-fold ($p < 0.01$) in ALS.

To further verify the localization and extent of expression of genes of interest, we performed in situ hy-

Table 5. Downregulated Genes in Spinal Ventral Horns of ALS (Bottom 30)

GeneBank	Gene Name	Fold Change (ALS/control)
NM_000843	Glutamate receptor, metabotropic 6	0.22
NM_000730	cholecystokinin A receptor	0.24
NM_003134	Signal recognition particle 14kDa	0.26
NM_003163	Syntaxin 1B	0.27
NM_006476	ATP synthase, H+ transporting, mitochondrial F1F0, subunit g	0.27
NM_001610	Acid phosphatase 2, lysosomal	0.28
NM_003108	SRY (sex determining region Y)-box 11	0.29
NM_001446	Fatty acid binding protein 7, brain	0.30
NM_004583	RAB5C, member RAS oncogene family	0.31
NM_001125	ADP-ribosylarginine hydrolase	0.31
NM_003320	Tubby (mouse) homolog	0.31
NM_001731	B-cell translocation gene 1, antiproliferative	0.31
NM_000999	Ribosomal protein L38	0.32
NM_004128	General transcription factor IIF, polypeptide 2 (30kDa subunit)	0.32
NM_001765	CD1C antigen, c polypeptide	0.32
NM_004430	Early growth response 3 (EGR3)	0.33
K00558	Tubulin, α, ubiquitous	0.33
NM_006732	FBJ murine osteosarcoma viral oncogene homolog B	0.33
NM_002040	GA-binding protein transcription factor, α subunit (60kDa)	0.34
NM_006161	Neurogenin 1	0.35
NM_002684	Postmeiotic segregation increased 2–like 11	0.35
NM_000801	FK506-binding protein 1A (12kDa)	0.35
NM_001051	Somatostatin receptor 3	0.35
NM_005017	Phosphate cytidylyltransferase 1, choline, alpha isoform	0.36
NM_004927	Chromosome 11 open reading frame 4	0.36
NM_000046	Arylsulfatase B	0.37
NM_004378	Cellular retinoic acid–binding protein 1 (CRABP1)	0.37
NM_001998	Fibulin 2	0.38
NM_001839	Calponin 3, acidic	0.38
NM_001183	ATPase, H+ transporting, lysosomal, subunit 1	0.39

Gene expression levels are expressed as means of fold-change, which is calculated by dividing the signals of each ALS sample by those of control samples, in the five patients with ALS.
ALS = amyotrophic lateral sclerosis.

bridization on selected genes. The mRNAs for acetyl-CoA transporter, KIAA0231, and EGR3 were localized in the remaining motor neurons (Fig 4). Spinal motor neurons overexpressed acetyl-CoA transporter and KIAA0231 in ALS, whereas EGR3 was underexpressed. Moreover, TrkC, CRABP1, Bak, and dynactin 1 gene expression was found in motor neurons, and those signals were reduced in ALS. DR5 signals were increased in motor neurons in ALS. Cyclin C signals with punctate immunoreactivity were increased in the cytoplasm as well as in nuclei in ALS motor neurons. The nuclear staining of motor neurons for cyclin C was more prominent in ALS compared with controls.

Discussion

Although reports about differential gene expression using the postmortem spinal cords, including those of patients with ALS, have been published,[26,27] the precise gene expression profiles of the degenerating motor neurons themselves have remained to be elucidated. Laser-captured dissection of motor neurons and subsequent microarray analysis are the most appropriate approaches to understanding the motor neuron–specific gene expression profile related to the motor neuron degeneration process in sporadic ALS, because these approaches eliminate bias of motor neuron loss, reactive astroglial proliferation, and other cellular reactions. Indeed, serine kinase has been reported to be underexpressed in ALS spinal cord gray matter,[27] but this study showed it was overexpressed in isolated motor neurons, suggesting that the reported underexpression in whole gray matter was influenced by the decreased motor neuron population. In contrast, cathepsin D expression was downregulated in the ALS motor neurons in this study, whereas it was increased in spinal cord gray matter in a previous report,[27] indicating its upregulation in glial cells. In addition, clustering analyses showed that the gene expression profile in the spinal motor neurons was substantially different from that in the whole homogenates of spinal ventral horn gray matter.

The overall microarray analysis using spinal ventral horn homogenates showed gene expression changes in less than 1% of genes examined with more genes showing increased than decreased expression. On the other hand, the motor neuron–specific microarray analysis

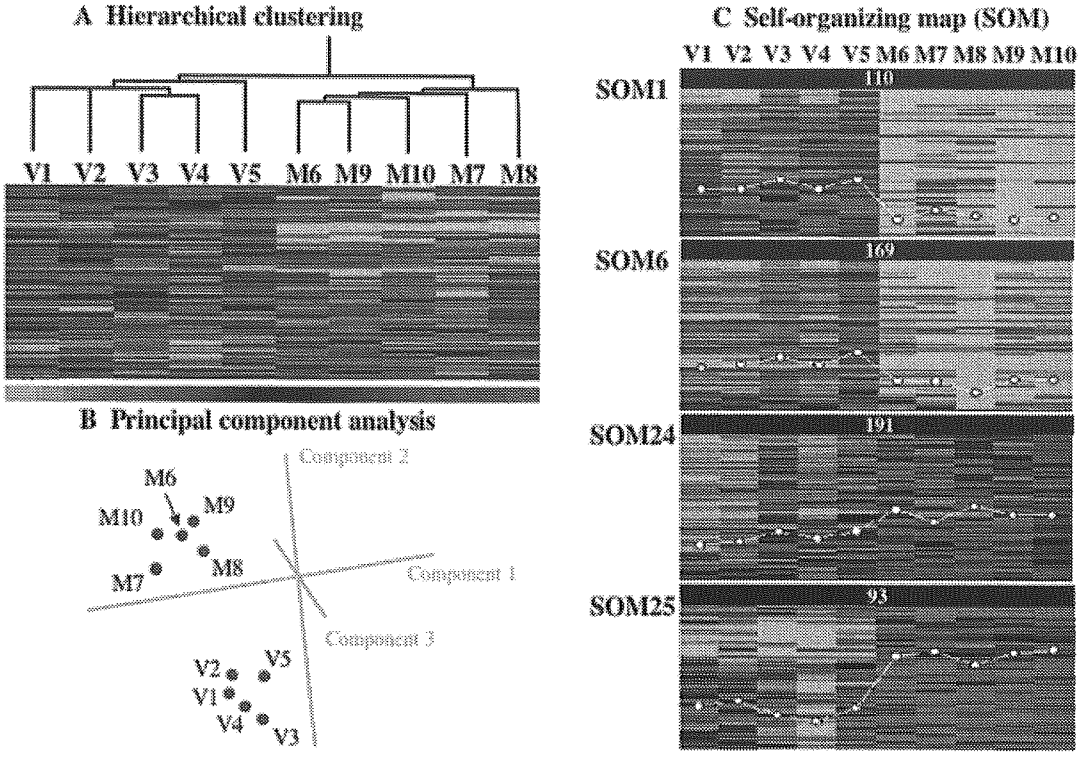

Fig 2. Clustering of gene expression in spinal motor neurons and spinal ventral horns. (A) Hierarchical clustering of gene expression in spinal motor neurons and ventral horns. The dendrogram was produced by hierarchical clustering of relative expression levels of 4,845 genes (rows) in five spinal homogenate and five motor neuron samples (columns) in making a total of 48,450 data points. Visual representation is shown with green representing downregulated (<0.44), black representing intermediate, and red representing upregulated (>2.28). The hierarchical clustering successfully detects two large clusters of amyotrophic lateral sclerosis (ALS), discriminating between spinal homogenates of ventral horns (samples V1 [ALS1], V2 [ALS10], V3 [ALS3], V4 [ALS14], and V5 [ALS13]) and motor neurons (samples M6 [ALS1], M7 [ALS10], M8 [ALS14], M9 [ALS11], and M10 [ALS7]), with a correlation coefficient of 0.446 at the branching point. (B) Principal component analysis of spinal motor neurons and ventral horns. Principal component analysis by six components for the 4,845 genes shows two main clusters consisting of spinal motor neurons (M6–10) and homogenates (V1–5). The number of patients corresponds to those in the dendrogram. (C) Self-organizing map (SOM) analysis of spinal motor neurons and ventral horns. The 4,845 genes are grouped into 25 clusters, the optimal size of which is calculated from gap statistics analysis. In SOM1 and SOM6, most genes are downregulated and in SOM24 and SOM25 the majority of genes are upregulated commonly in isolated motor neurons of five cases (M6–10). The numbers of genes are given at the top, and selected genes are listed for clusters 1, 6, 24, and 25 in Table 6.

showed that the proportion of significantly downregulated genes was 3% of the examined genes, whereas that of upregulated genes was one third of the downregulated genes. Moreover, the genes found to be downregulated specifically in motor neurons were not found to be downregulated in ventral horns, except for three genes with high expression levels. These results strongly support the notion that microarray analysis of laser-captured isolated spinal motor neurons has an advantage especially for the detection of motor neuron–specific downregulated transcripts.

In the differentially expressed genes, cell death–associated genes and genes related to cell signaling were characteristically upregulated in ALS motor neurons, whereas the genes categorized into cytoskeleton and transcription were downregulated. In the prominently altered genes of interest related to the cell death pathway, acetyl-coenzyme A transporter, which has been cloned and shown to encode a protein with multitransmembranous spanning domains,[28] was overexpressed in ALS motor neurons. Acetyl-CoA transporter functions as a cofactor for acetylation of gangliosides as well as vesicular transport of acetylcholine, which is synthesized from acetyl-CoA and choline. Acetylation has been documented to suppress proapoptotic activity of GD3 ganglioside, which increased in ALS neural tissues, as previously shown.[29,30] These results suggest that enhanced expression of acetyl-CoA transporter may be related to the antiapoptotic mechanism for cholinergic motor neuron degeneration in ALS.

Table 6. Selected Genes Characterized by SOM (select each 15)

GeneBank	Gene Name	Fold Change (ALS/control)
SOM1/6: genes downregulated in ALS motor neurons		
NM_002695	Polymerase (RNA) II (DNA directed) polypeptide E (25kD)	0.20
M24857	Retinoic acid receptor gamma 1 (RAR-γ 1)	0.20
NM_002375	Microtubule-associated protein 4	0.20
NM_001651	Aquaporin 5	0.21
NM_003178	Synapsin II	0.22
NM_004624	Vasoactive intestinal peptide receptor 1	0.23
NM_001740	Calbindin 2, (29kD, calretinin)	0.24
M73812	G1/S-specific cyclin E (CCNE)	0.25
NM_003206	Transcription factor 21	0.25
NM_004082	Dynactin 1 (p150)	0.30
U05012	TRK-C; NT-3 growth factor receptor precursor	0.31
NM_003632	Contactin associated protein 1	0.32
NM_005910	Microtubule-associated protein tau	0.49
NM_002373	Microtubule-associated protein 1A	0.51
NM_002442	Musashi (Drosophila) homolog 1	0.52
SOM24/25: genes upregulated in ALS motor neurons		
M60718	Hepatocyte growth factor (HGF)	3.42
L20814	Glutamate receptor subunit 2 (GLUR-2)	3.34
K02268	β-neoendorphin-dynorphin precursor	3.13
L19063	Glial cell line–derived neurotropic factor (GDNF)	3.08
NM_005543	Insulin-like 3	2.79
J04088	DNA topoisomerase II alpha (TOP2A)	2.58
M22489	Bone morphogenetic protein 2A (BMP2A)	2.57
U51004	Hint protein; protein kinase C inhibitor	2.26
M87507	Caspase 1, interleukin-1 β convertase precursor	2.21
NM_006196	Poly(rC)-binding protein 1	2.16
L29511	Growth factor receptor–bound protein 2	2.04
U78798	TRAF6	1.98
NM_001229	Caspase 9, apoptosis-related cysteine protease	1.89
U84388	Caspase and rip adaptor with death domain (CRADD)	1.83
U13737	Caspase-3	1.77

Gene expression levels are expressed as means of fold-change, which is calculated by dividing the signals of each ALS sample by those of control samples, in the five patients with ALS. Genes listed in Tables 2 and 3 are excluded.
SOM = self-organizing map.

KIAA0231 was one of the mostly overexpressed genes in ALS motor neurons, but the function of this gene product is not known.

In the greatly downregulated genes of interest related to transcription, EGR3, whose expression was remarkably reduced in motor neurons of ALS, is a zinc-finger immediate-early transcription factor that is important for neurotrophin-3 (NT-3) regulation. It is known that EGR3 knockout mice develop gait ataxia, scoliosis, resting tremors, and ptosis due to the degeneration of muscle spindles, through disruption of NT-3 regulation.[31] In ALS motor neurons, TrkC receptor for NT-3 was underexpressed, whereas NT-3 expression was not changed. The finding about TrkC-null mutant and NT-3–null mutant mice show that NT-3-TrkC signaling is required to maintain Ia afferent central synapses of DRG neurons.[32] The marked downregulation of EGR3 in spinal motor neurons may disrupt sensory-motor connections by decreasing NT-3-TrkC signaling, resulting in motor neuron degeneration.

For neurotrophic support for ALS motor neurons, this study showed the overexpression of CNTF, GDNF, and HGF involved in the functional category of cell signaling, suggesting that these neurotrophic factors would be secondarily and compensatorily upregulated after motor neuron degeneration. Indeed, GDNF expression has been reported to increase in the spinal cords and decrease in the muscles of sporadic ALS patients.[33] In contrast with these neurotrophic factors, midkine was one of the significantly downregulated neurotrophic factors. Because midkine plays important roles in promotion of neuronal survival as well as modulation of neuromuscular junctions,[34] its underexpression may be related to motor neuron degeneration. In addition, the gene expression of vascular endothelial growth factor, which has been identified as a critical factor for motor neuron degeneration,[35–37] did not change significantly in gene expression in this study. SOD1 gene expression was not altered in spinal motor neurons and ventral horns. Moreover, the gene expres-

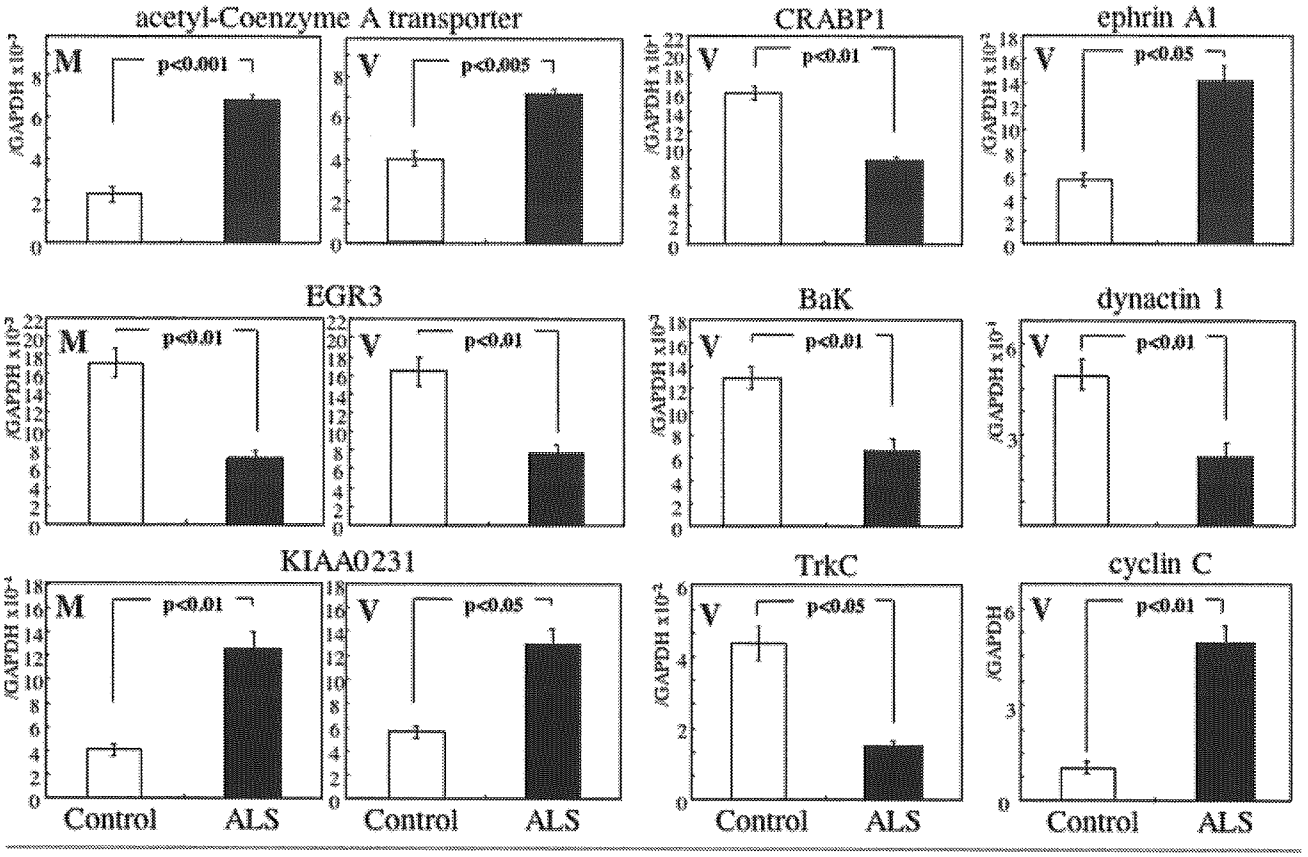

Fig 3. Quantitative real-time reverse transcription polymerase chain reaction verification of the selected genes. Expression levels of acetyl-coenzyme A transporter, EGR3, KIAA0231, CRABP1, Bak, TrkC, ephrin A1, cyclin C, dynactin 1, and GAPDH were measured using spinal motor neurons (M) and ventral horns (V), and those of the target genes were normalized against the GAPDH level. The relative expression levels are expressed as mean ± standard error for 13 amyotrophic lateral sclerosis (ALS) cases and 11 controls. Gene names (Genebank accession number), primers and probe sequences (forward primer, reverse primer, and TaqMan probe; 5' to 3' sequence) were as follows: [acetyl-CoA transporter: D88152] (GGGTTACTTTTTGGGCAATG, AACGATTCCTCTGGGTTGAG, FAM-TTGGCCCTTGAATCTGCCGA-TAMRA); [Bak: NM_001188] (CTGGAAGATCAGCACCCTAAG, CCCCTCTCCTAGTAGGTCCTG, FAM-TGCTCCCATTCCTCCCTCCG-TAMRA); [CRABP1: NM_004378] (TGCAGGAGTTTAGCCACTTG, CTCACGGGTCCAGTAGGTTT, FAM- TGAGAACAAGATCCACTGCACCCA-TAMRA); [cyclin C: M74091] (TGAGCAGTGGAAGAATTTCG, ACCCTGCTCTCCTTCACTGT, FAM- TGCCAAAACCAAAACCACCTCCA-TAMRA); [dynactin 1: NM_004082] (ATGTGAATCGGGAACTGACA, GGGCCTTAGTCTCAGCAAAC, FAM- TGGAGAGGCAACAGCAGCCAC-TAMRA); [EGR3: NM_004430] (CTTCCCCATGATTCCTGACT, TTGAATGCCTTGATGGTCTC, FAM-TTCCAGGGCATGGACCCCAT-TAMRA); [ephrin A1: M57730] (GGCAAGGAGTTCAAAGAAGG, TCACCTTCAACCTCAAGCAG, FAM- CCATCCACCAGCATGAAGACCG-TAMRA); [GAPDH: NM_002046] (TCAAGAAGGTGGTGAAGCAG, GGTGTCGCTGTTGAAGTCAG, FAM-CCTCAAGGGCATCCTGGGCT-TAMRA); [KIAA0231: D86984] (CAACGGTCTTCCAGACAATG, GAGGTTGACCAGCTGTGAGA, FAM-TCCCAGAGGTGAAGCTGCCCTCTAMRA); and [TrkC: U05012] (TGAGAACCCCCAGTACTTCC, TCAGCACGATGTCTCTCCTC, FAM-CTGCCACAAGCCGGACACGT-TAMRA).

sion level of GluR2 was upregulated, as shown by its classification in SOM25, but the expression of its editing enzyme (adenosine deaminase, RNA-specific, 2; ADAR2) was not altered in this study, although the editing efficiency of GluR2 mRNA has been demonstrated to be low in spinal motor neurons of ALS.[38]

Genes subject to transcriptional regulation constitute a crucial part of the whole human genome as demonstrated by human genome projects.[39] In addition to the gene expression of EGR3, the gene expression of retinoic acid receptor α and γ together with cellular retinoic acid–binding protein 1 (CRABP1), and Musashi 1, all of which are known to be inducers of neuronal differentiation,[40,41] was downregulated in spinal motor neurons of ALS. The dysregulation of retinoid receptor and retinol binding protein has been reported in the postmortem spinal cords of ALS and SOD1 mutant mice.[17,26] These interesting results imply the potential involvement of the differentiation signals in maintaining motor neuron integrity, which

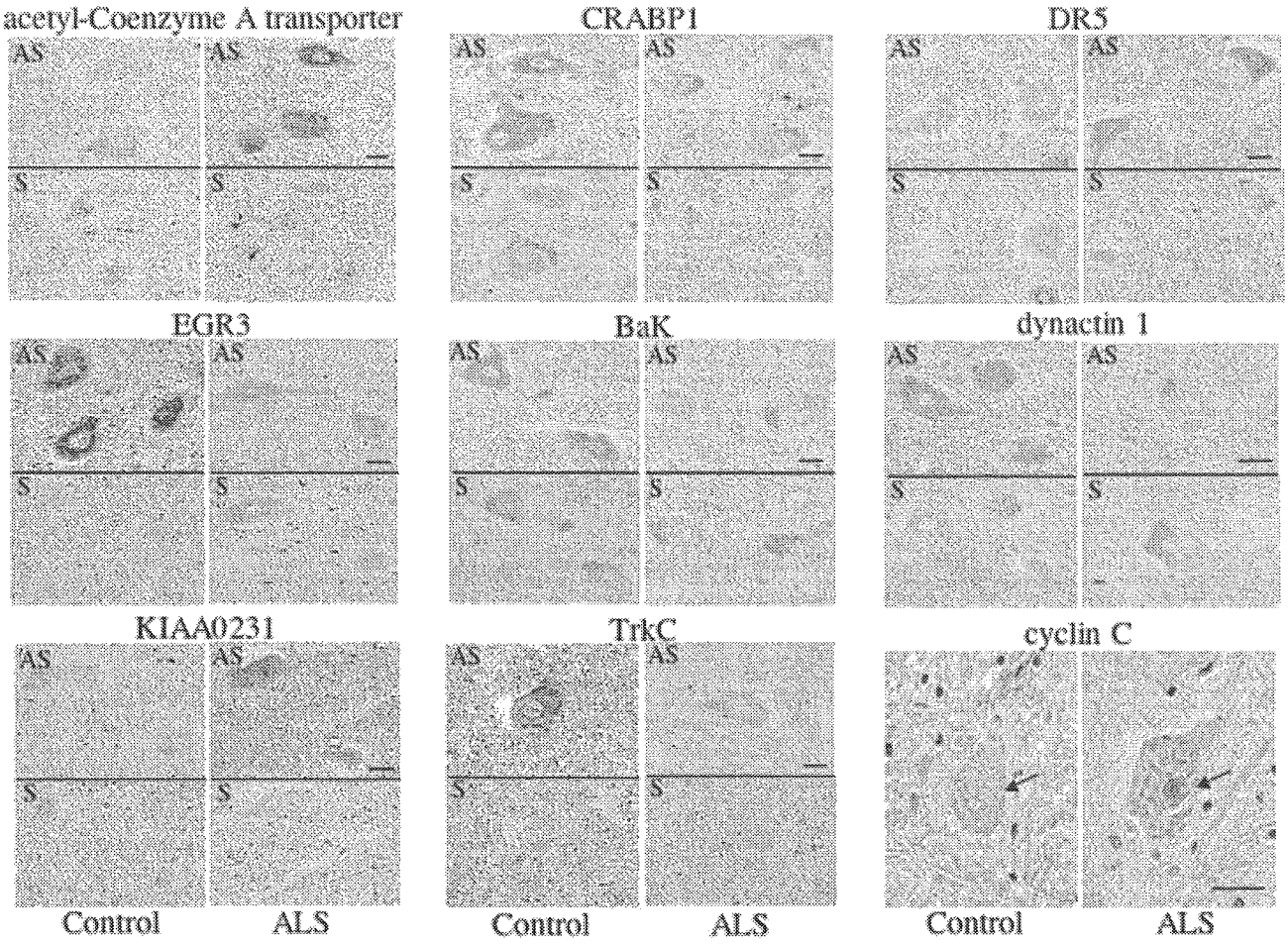

Fig 4. In situ hybridization and immunohistochemistry of the selected genes. Representative in situ hybridization is shown for acetyl-COENZYMEA transporter, EGR3, KIAA0231, CRABP1, Bak, TrkC, DR5, and dynactin 1. The antisense probe (AS) detects positive signals for the expression of each gene in spinal motor neurons for ALS and/or controls, but the sense probe (S) does not. Lipofuscin granules are seen as yellowish granules. Immunohistochemistry was preformed for cyclin C, and nuclear staining was prominent in ALS motor neurons. Arrows denote the nuclei. Bars = 25μm.

might be impaired in the neurodegenerative process of ALS. Among the genes related to transcriptional regulation, the number of significantly downregulated genes was twofold greater than that of the upregulated ones in ALS motor neurons. These downregulated transcription-related genes were not restricted to genes regulating neuronal differentiation as neuron-specific cellular properties, but also included genes such as RNA polymerase and transcription factors, which regulate general cellular functions. These observations suggest that downregulation of transcriptional activity may be the reflection of motor neuron dysfunction because of a wide range of impairments of cellular maintenance systems.

Interestingly, the expression of dynactin 1, which recently has been identified as a causative gene for human motor neuron disease,[42] was reduced in ALS motor neurons. Some other motor proteins including the kinesin family responsible for antegrade axonal transport and dyneins for retrograde axonal transport were not changed significantly, but the expression levels of MAPs 1A, 4, and tau were decreased, shown by their classification in SOM1 and SOM6. The impairment of axonal transport is thought to be an early event of motor neuron degeneration, and especially the protein levels of MAPs 1A and tau have been reported to decrease early before the onset of symptoms in mutant SOD1 transgenic mice.[43–45] The upregulation of ubiquitin-specific protease 11 (USP11), listed in Tables 2 and 3, also may be related to microtubule abnormality because the RanGTP-associated protein RanBPM, which is required for correct nucleation of microtubules, is the enzymatic substrate for USP11.[46] The present results imply that retrograde axonal transport, especially that associated with dynactin, might be affected even at the terminal stage of ALS and be crucial for motor neurons, although cytoskeletal proteins are the major functional group in the downregulated genes.